

Nucleon-Nucleon Effective Field Theory Without Pions

Jiunn-Wei Chen^a, Gautam Rupak^a and Martin J. Savage^{a,b}

^a *Department of Physics, University of Washington, Seattle, WA 98915.*

^b *Jefferson Lab., 12000 Jefferson Avenue, Newport News, Virginia 23606.*

Abstract

Nuclear processes involving momenta much below the mass of the pion may be described by an effective field theory in which the pions do not appear as explicit degrees of freedom. The effects of the pion and all other virtual hadrons are reproduced by the coefficients of gauge-invariant local operators involving the nucleon field. Nucleon-nucleon scattering phase shift data constrains many of the coefficients that appear in the effective Lagrangean but at some order in the expansion coefficients enter that must be constrained by other observables. We compute several observables in the two-nucleon sector up to next-to-next-to leading order in the effective field theory without pions, or to the order at which a counterterm involving four-nucleon field operators is encountered. Effective range theory is recovered from the effective field theory up to the order where relativistic corrections enter or where four-nucleon-external current local operators arise. For the deuteron magnetic moment, quadrupole moment and the $np \rightarrow d\gamma$ radiative capture cross section a four-nucleon-one-photon counterterm exists at next-to-leading order. The electric polarizability and electric charge form factor of the deuteron are determined up to next-to-next-to-leading order, which includes the first appearance of relativistic corrections.

February 1999

I. INTRODUCTION

Weinberg's pioneering work [1] on the application of effective field theory (EFT) to nuclear physics has given rise to a decade long effort to construct a perturbative theory of nuclear interactions [2]- [31]. The small kinetic and potential energies of nuclear systems compared to the typical scale of strong interactions, either Λ_{QCD} or the chiral symmetry breaking scale Λ_χ , suggests that the ratio of these two scales might provide a small expansion parameter. Indeed, in the single nucleon sector the ratio of external momenta and quark masses, m_q , to Λ_χ allows for a systematic field theory description of pionic and external current interactions with a single nucleon. However, extending this simple idea to multi-nucleon systems has proved to be a challenge.

It is important to understand nuclear physics directly from quantum chromodynamics (QCD) and constructing the correct low-energy effective field theory is a central component of such a program. The optimal way to determine the properties of multi-nucleon systems is to match onto the low-energy effective field theory and perform computations directly with the effective theory, and not with the theory written in terms of quark and gluon fields. Further, one wants to be able to make such a matching between QCD and the low-energy effective theory free of any unjustified assumptions about the dynamics or structure of the hadrons. Unfortunately, at this point in time such a matching is not possible. However, the symmetries of QCD along with the fact that we wish to examine observables involving small external momenta allow the low-energy effective field theory to relate the amplitudes of different strong interaction processes, at some level of precision.

Significant progress in understanding both the two-body and three-body systems in terms of effective field theory has been made during the last year. Several observables in the two-nucleon sector have been explored in detail in the theory with dynamical pions, such as the electromagnetic form factors of the deuteron [12], $\gamma d \rightarrow \gamma d$ [13,14], $np \rightarrow d\gamma$ [16,17,24] and $\nu d \rightarrow \nu d, \nu np$ [30]. In addition, the inclusion of coulomb interactions into the pionless theory has been shown to be straightforward [26]. In the three-nucleon system it has been demonstrated that low-momentum processes can be accurately and precisely described in the effective field theory without dynamical pions [31]. For example the quartet $N - d$ scattering length has a rapidly converging expansion in terms of the ratio $r_0^{(3S_1)}/a^{(3S_1)}$, where $r_0^{(3S_1)}$ is the effective range and $a^{(3S_1)}$ is the scattering length for NN scattering in the spin-triplet channel. Calculations in the two-nucleon sector [12–17] with dynamical pions using the KSW power counting scheme [10], (where pions and higher dimension four-nucleon operators are treated in perturbation theory) have been performed at leading order (LO) and next-to-leading order (NLO), and just recently been extended in some cases to next-to-next-to-leading (NNLO) [18,19].

In this work we make a thorough investigation of the two-nucleon sector in the theory without dynamical pions, appropriate for very low-momentum processes. Effective range theory [32] is found to reproduce the effective field theory up to the order where relativistic corrections or local four-nucleon-external-current local operators enter. In many cases effective field theories for hadronic systems are used to systematically include the approximate $SU(2)_L \otimes SU(2)_R$ chiral symmetry of QCD. As we are considering the theory of nucleon interactions where pions do not explicitly appear, chiral symmetry does not play a central role and the usefulness of this investigation could be questioned. One motivation for con-

structuring and understanding this theory is that calculations of the observables considered in this work with any scheme, such as potential models or the effective field theory with dynamical pions, must reproduce the analytic results we obtain. A secondary motivation is that this theory provides a very clear demonstration of how the perturbative effective field theory approach to NN interactions behaves at higher orders, including relativistic effects.

II. NN SCATTERING IN THE ${}^3S_1 - {}^3D_1$ CHANNEL

The large scattering lengths in the two-nucleon system require a modification of the power counting rules that follow naturally from the single nucleon sector in order to describe multi-nucleon processes. For processes in which all external momenta are much below the mass of the pion ($|\mathbf{k}| \ll m_\pi$) it is desirable to use an EFT without pions, which we denote by EFT($\not{\pi}$). The external momenta divided by the pion mass is the small expansion parameter of this theory, denoted by Q . As there are no dynamical pions, all quark mass effects are reproduced by local operators involving two or more nucleons and an arbitrary number of spatial derivatives. EFT($\not{\pi}$) has the same power counting as effective range theory where the relative momentum of the nucleons in the two-body NN system is treated as the small expansion parameter. However, EFT($\not{\pi}$) includes operators with insertions of arbitrary numbers of external currents, that are not constrained by NN scattering phase shifts alone.

Let us recall the low-momentum behavior of the phase shift in a system with a large scattering length. We know from elementary scattering theory that $|\mathbf{k}| \cot \delta_0$ is an analytic function of external kinetic energy with a radius of convergence bounded by the threshold for pion exchange in the t-channel, and thus

$$|\mathbf{k}| \cot \delta_0 = -\frac{1}{a} + \frac{1}{2}r_0|\mathbf{k}|^2 + r_1|\mathbf{k}|^4 + \dots, \quad (2.1)$$

where we have chosen to write the expansion in terms of the center of mass momentum $|\mathbf{k}|$. One is free to expand $|\mathbf{k}| \cot \delta_0$ about any point within the region of convergence, and eq. (2.1) corresponds to expanding about $|\mathbf{k}| = 0$. The size of the coefficients r_0, r_1, \dots is set by the range of the interaction between the nucleons, of order the pion mass, and the r_i are taken to scale as Q^0 in the power counting. In contrast, the scattering length a is not constrained by the range of the underlying interaction. The scattering lengths for NN scattering in both the 1S_0 and 3S_1 channel are very much larger than the inverse pion mass, and are taken to scale as $a \sim Q^{-1}$ in the power counting. In dealing with the deuteron bound state, it is convenient to make the expansion of $|\mathbf{k}| \cot \delta_0$ about the location of the deuteron pole [32], and not about $|\mathbf{k}| = 0$. Expanding around the deuteron pole, $|\mathbf{k}|^2 = -\gamma_t^2$ gives

$$\begin{aligned} |\mathbf{k}| \cot \delta_0 &= -\gamma_t + \frac{1}{2}\rho_d(|\mathbf{k}|^2 + \gamma_t^2) + w_2 (|\mathbf{k}|^2 + \gamma_t^2)^2 + \dots \\ &= \mathcal{O}(Q) + \mathcal{O}(Q^2) + \mathcal{O}(Q^4) + \dots, \end{aligned} \quad (2.2)$$

with $\gamma_t^{-1} = 4.318946$ fm, $\rho_d = 1.764$ fm, and $w_2 = 0.389$ fm³ [33]. The total energy of each nucleon in the center of mass is $\overline{E}_N = \sqrt{|\mathbf{k}|^2 + M_N^2}$, and the deuteron pole is located at $|\mathbf{k}| = i\gamma_t$, the solution to

$$-B = 2\sqrt{M_N^2 - \gamma_t^2} - 2M_N \quad , \quad (2.3)$$

where $B = 2.224575$ MeV is the deuteron binding energy. Subsequently, we will find it convenient to work with the parameter $\gamma = \sqrt{M_N B}$, which is related to γ_t , by a Q expansion of eq (2.3),

$$\gamma = \gamma_t + \frac{\gamma_t^3}{8M_N^2} + \dots \quad . \quad (2.4)$$

The S-matrix describing scattering in the coupled channel $J = 1$ system is written as

$$S = \begin{pmatrix} e^{i2\delta_0} \cos 2\bar{\varepsilon}_1 & ie^{i(\delta_0+\delta_2)} \sin 2\bar{\varepsilon}_1 \\ ie^{i(\delta_0+\delta_2)} \sin 2\bar{\varepsilon}_1 & e^{i2\delta_2} \cos 2\bar{\varepsilon}_1 \end{pmatrix} \quad , \quad (2.5)$$

where we use the ‘‘barred’’ parameterization of [34], also used in [33]. It will follow naturally from the EFT(\mathcal{F}) that $\bar{\varepsilon}_1$ is suppressed by Q^2 compared with $\delta_0^{(0)}$, and therefore, up to N⁴LO, we can isolate the S-wave from the D-wave in the deuteron channel, leaving

$$S_{00} = e^{i2\delta_0} = 1 + \frac{2i}{\cot \delta_0 - i} \quad . \quad (2.6)$$

The phase shift δ_0 has an expansion in powers of Q , $\delta_0 = \delta_0^{(0)} + \delta_0^{(1)} + \delta_0^{(2)} + \dots$, where the superscript denotes the order in the Q expansion. By forming the logarithm of both sides of eq. (2.6) and expanding in powers of Q , it is straightforward to obtain

$$\begin{aligned} \delta_0^{(0)}(|\mathbf{k}|) &= \pi - \tan^{-1} \left(\frac{|\mathbf{k}|}{\gamma} \right) \\ \delta_0^{(1)}(|\mathbf{k}|) &= -\frac{\rho_d}{2} |\mathbf{k}| \\ \delta_0^{(2)}(|\mathbf{k}|) &= - \left[\frac{\rho_d^2 \gamma}{4} + \frac{\gamma^3}{8M_N^2(\gamma^2 + |\mathbf{k}|^2)} \right] |\mathbf{k}| \quad , \end{aligned} \quad (2.7)$$

which are shown in fig. (1). Up to NNLO, the shape parameter term, w_2 does not contribute to the S-wave phase shift and therefore, in addition to being numerically small (about a factor of 5 smaller than ρ_d), w_2 enters only at high orders. Formally, the first deviations from linear $|\mathbf{k}|$ dependence at large momenta arise from relativistic corrections (the second term in $\delta_0^{(2)}$ in eq. (2.7)). The Q expansion is clearly demonstrated in eq. (2.7), by simply counting powers of $|\mathbf{k}|$ and γ , which both scale like Q . We expect that this perturbative expansion of the phase shifts converges up to momenta of order $\sim m_\pi/2 \sim 70$ MeV, at which point one encounters the t-channel cut from potential pion exchange. In the theory where pions are dynamical, the range of convergence of the theory is much beyond the scale set by the pion mass. An analogous expression for the perturbatively expanded S-wave phase shift that is valid up to momenta of order ~ 300 MeV at NLO can be found in [10].

This simple perturbative expansion of the phase shift and scattering amplitude is reproduced order by order in the EFT(\mathcal{F}) expansion. Relativistic corrections are encountered at NNLO and therefore a discussion of the nucleon two-point function is appropriate. The total energy of a nucleon E_N and its kinetic energy T_N are simply related by $E_N = M_N + T_N$. A nucleon propagator can be written in terms of T_N and the nucleon three momentum \mathbf{p} ,

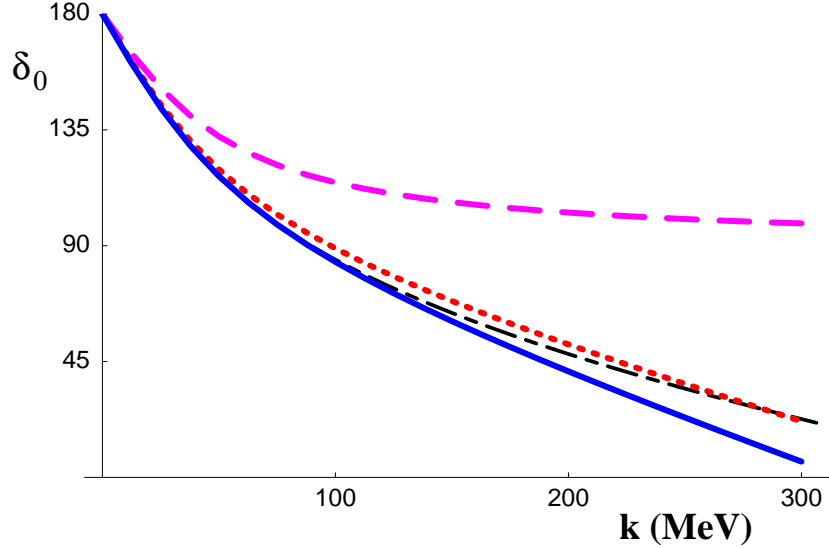


FIG. 1. The phase shift δ_0 as a function of the center of mass momentum $|\mathbf{k}|$. The dashed curve corresponds to $\delta_0^{(0)}$, the dotted curve corresponds to $\delta_0^{(0)} + \delta_0^{(1)}$, the solid curve corresponds to $\delta_0^{(0)} + \delta_0^{(1)} + \delta_0^{(2)}$, and the dot-dashed curve is the Nijmegen partial wave analysis [35].

$$\begin{aligned} \frac{i(\not{p} + M_N)}{p^2 - M_N^2} &= \frac{2iM_N}{(M_N + T_N)^2 - |\mathbf{p}|^2 - M_N^2 + i\epsilon} \\ &= \frac{2iM_N}{2M_N T_N + T_N^2 - |\mathbf{p}|^2 + i\epsilon} \quad , \end{aligned} \quad (2.8)$$

and is reproduced by a Lagrange density involving the nucleon field N with the time-dependent phase corresponding to the nucleon mass removed,

$$\mathcal{L} = N^\dagger \left[i\partial_0 + \frac{\nabla^2}{2M_N} - \frac{\partial_0^2}{2M_N} \right] N + \dots \quad . \quad (2.9)$$

In the EFT(π) we treat the third term in eq. (2.9) as a perturbation and it is not resummed into the nucleon propagator. In order to recover the usual nonrelativistic expansion of the two-point function, a field redefinition is employed followed by use of the equations of motion [36], e.g.

$$N' = \left(1 - \frac{\nabla^2}{4M_N^2} + \dots \right) N \quad , \quad (2.10)$$

gives

$$\mathcal{L} = N'^\dagger \left[i\partial_0 + \frac{\nabla^2}{2M_N} + \frac{\nabla^4}{8M_N} + \dots \right] N' + \dots \quad . \quad (2.11)$$

It is somewhat inconvenient to use this second form of the Lagrangean due to the fact that the field redefinition in eq. (2.10) must be performed on all terms in the Lagrange density describing the NN systems including the multi-nucleon interactions.

The inclusion of electromagnetic interactions requires that ∇ operators be replaced by covariant derivatives $\mathbf{D} = \nabla - ie\mathbf{A}$, and time-derivatives ∂_0 be replaced by $D_0 = \partial_0 + ieA_0$. The Lagrange density describing the interaction between two nucleons scattering in the 3S_1 channel written in terms of one-body \mathcal{L}_1 and two-body \mathcal{L}_2 interactions, and up to NNLO, is

$$\begin{aligned}\mathcal{L}_1 &= N^\dagger \left[iD_0 + \frac{\mathbf{D}^2}{2M_N} - \frac{D_0^2}{2M_N} \right] N \\ \mathcal{L}_2 &= -\not{C}_0^{(3S_1)} \left(N^T P_i N \right)^\dagger \left(N^T P_i N \right) \\ &\quad + \not{C}_2^{(3S_1)} \frac{1}{8} \left[\left(N^T P_i N \right)^\dagger \left(N^T \left[P_i \vec{\mathbf{D}}^2 + \overleftarrow{\mathbf{D}}^2 P_i - 2\overleftarrow{\mathbf{D}} P_i \vec{\mathbf{D}} \right] N \right) + h.c. \right] \\ &\quad - \frac{1}{16} \not{C}_4^{(3S_1)} \left(N^T \left[P_i \vec{\mathbf{D}}^2 + \overleftarrow{\mathbf{D}}^2 P_i - 2\overleftarrow{\mathbf{D}} P_i \vec{\mathbf{D}} \right] N \right)^\dagger \left(N^T \left[P_i \vec{\mathbf{D}}^2 + \overleftarrow{\mathbf{D}}^2 P_i - 2\overleftarrow{\mathbf{D}} P_i \vec{\mathbf{D}} \right] N \right) \quad (2.12)\end{aligned}$$

where P_i is the spin-isospin projector for the 3S_1 channel

$$P_i \equiv \frac{1}{\sqrt{8}} \sigma_2 \sigma_i \tau_2 \quad , \quad \text{Tr } P_i^\dagger P_j = \frac{1}{2} \delta_{ij} \quad . \quad (2.13)$$

The subscript on the coefficient denotes the number of derivatives in the operator. There is another operator involving four derivatives that we have not shown in eq. (2.12),

$$\mathcal{L} = -\frac{1}{32} \not{\tilde{C}}_4^{(3S_1)} \left[\left(N^T (\overleftarrow{\mathbf{D}} - \vec{\mathbf{D}})^4 P_i N \right)^\dagger \left(N^T P_i N \right) + h.c. \right] \quad , \quad (2.14)$$

(we have not shown the correct ordering of the P_i and \mathbf{D} operators). Renormalization group scaling [10] of the operators in eq. (2.12) and eq. (2.14) indicates that while the contribution from $\not{C}_4^{(3S_1)}$ is NNLO, the contribution from $\not{\tilde{C}}_4^{(3S_1)}$ is N³LO. The time-ordered product of two $\not{C}_2^{(3S_1)}$ operators does not induce the momentum structure of the $\not{\tilde{C}}_4^{(3S_1)}$ operator.

The effective range expansion provides a complete description of scattering in the low energy region. It is straightforward to show that the relation between the expansion of $\cot \delta_0$ and the coefficients in eq. (2.12) is,

$$-|\mathbf{k}| \cot \delta_0 = \frac{2\pi \bar{E}}{M_N^2} \frac{1}{\sum \not{C}_{2n} |\mathbf{k}|^{2n}} + \mu \quad , \quad (2.15)$$

where μ is the dimensional regularization renormalization scale, explicitly introduced by the PDS subtraction procedure [10].

$$\bar{E} = 2M_N + \bar{T} = 2M_N + \frac{|\mathbf{k}|^2}{M_N} - \frac{|\mathbf{k}|^4}{4M_N^3} + \dots \quad , \quad (2.16)$$

is the center of mass total energy of the two nucleon system, where each nucleon has kinetic energy $\frac{\bar{T}}{2}$, and momentum of magnitude $|\mathbf{k}|$. Lorentz invariance ensures that for two nucleons moving with total momentum \mathbf{P} and kinetic energy T , these quantities are related to the center of mass quantities by

$$T + \frac{T^2}{4M_N} - \frac{|\mathbf{P}|^2}{4M_N} = \bar{T} + \frac{\bar{T}^2}{4M_N} \quad . \quad (2.17)$$

Notice that in eq. (2.2) momentum independent terms appear at each order in the Q expansion, as the momentum expansion is about the deuteron pole and not about $\mathbf{k} = 0$ (further, one sees contributions from all powers of $|\mathbf{k}|^2$, up to a maximum order dictated by Q). Consequently, for the effective field theory to reproduce the effective range expansion, the coefficients appearing in eq. (2.12) will have an analogous expansion in powers of Q , e.g.

$$\begin{aligned}\not\#C_0^{(3S_1)} &= \not\#C_{0,-1}^{(3S_1)} + \not\#C_{0,0}^{(3S_1)} + \not\#C_{0,1}^{(3S_1)} + \dots \\ \not\#C_2^{(3S_1)} &= \not\#C_{2,-2}^{(3S_1)} + \not\#C_{2,-1}^{(3S_1)} + \dots \\ \not\#C_4^{(3S_1)} &= \not\#C_{4,-3}^{(3S_1)} + \dots \quad .\end{aligned}\tag{2.18}$$

The second subscript on each coefficient denotes the powers of Q in the coefficient itself. Relating terms order by order in the \mathbf{k} expansion of eq. (2.2) and eq. (2.15) we find that

$$\begin{aligned}\not\#C_{0,-1}^{(3S_1)} &= -\frac{4\pi}{M_N} \frac{1}{(\mu - \gamma)} = -5.586 \text{ fm}^2 \\ \not\#C_{0,0}^{(3S_1)} &= \frac{2\pi}{M_N} \frac{\rho_d \gamma^2}{(\mu - \gamma)^2} = 0.559 \text{ fm}^2 \\ \not\#C_{0,1}^{(3S_1)} &= -\frac{\pi}{M_N} \frac{\rho_d^2 \gamma^4}{(\mu - \gamma)^3} + \frac{\pi}{2M_N} \frac{\gamma^3}{M_N^2 (\mu - \gamma)^2} = -0.055 \text{ fm}^2 \\ \not\#C_{2,-2}^{(3S_1)} &= \frac{2\pi}{M_N} \frac{\rho_d}{(\mu - \gamma)^2} = 10.420 \text{ fm}^4 \\ \not\#C_{2,-1}^{(3S_1)} &= -\frac{2\pi}{M_N} \frac{\rho_d^2 \gamma^2}{(\mu - \gamma)^3} - \frac{2\pi}{M_N} \frac{1}{M_N^2 (\mu - \gamma)} = -2.210 \text{ fm}^4 \\ \not\#C_{4,-3}^{(3S_1)} &= -\frac{\pi}{M_N} \frac{\rho_d^2}{(\mu - \gamma)^3} = -19.440 \text{ fm}^6 \quad ,\end{aligned}\tag{2.19}$$

where the $1/M_N^2$ terms that do not depend upon ρ_d are relativistic corrections. We have chosen to renormalize the theory at $\mu = m_\pi$. Strictly speaking we should choose a much lower scale $\mu \sim Q$, but the RG invariance allows us to renormalize at any scale once we have established the power counting. The hierarchy between coefficients of the same operator but of different orders in the Q expansion is clear. It is straightforward to show that these coefficients reproduce the perturbatively expanded phase shift in eq. (2.7).

The amplitude that one computes from Feynman diagrams is simply related to the S-matrix. Explicit computation of Feynman diagrams, in an arbitrary frame, gives

$$A_{NR} = \frac{2\pi \bar{E}}{M_N^2} \frac{1}{|\mathbf{k}| \cot \delta - i|\mathbf{k}|} \quad ,\tag{2.20}$$

which is related to the S-matrix by

$$S = 1 + \frac{2i}{\cot \delta - i} = 1 + i \frac{|\mathbf{k}| M_N^2}{\pi \bar{E}} A_{NR} \quad .\tag{2.21}$$

In the process of computing the S-matrix from the Feynman diagrams, we have used the following S-wave states (consistent with the sign convention of [34])

$$|1, a; \mathbf{P}, |\mathbf{k}\rangle_{L=0} = \frac{1}{\sqrt{4\pi}} \frac{|\mathbf{k}|}{(2\pi)^3} \int d\Omega_{\mathbf{k}} \left[N_{\frac{\mathbf{P}}{2}-\mathbf{k}}^T P^a N_{\frac{\mathbf{P}}{2}+\mathbf{k}} \right]^\dagger |0\rangle \quad , \quad (2.22)$$

for the $J = 1, J_Z = a$ and $L = 0$ NN state. \mathbf{P} is the momentum of the center of mass of the NN system. Similarly, for the D-wave states,

$$|1, a; \mathbf{P}, |\mathbf{k}\rangle_{L=2} = -\frac{3}{\sqrt{8\pi}} \frac{1}{|\mathbf{k}|} \frac{1}{(2\pi)^3} \int d\Omega_{\mathbf{k}} \left[\mathbf{k}^x \mathbf{k}^a - \frac{1}{3} \delta^{ax} |\mathbf{k}|^2 \right] \left[N_{\frac{\mathbf{P}}{2}-\mathbf{k}}^T P^x N_{\frac{\mathbf{P}}{2}+\mathbf{k}} \right]^\dagger |0\rangle \quad , \quad (2.23)$$

where the $-ve$ sign gives the correct phase for the mixing parameter $\bar{\varepsilon}_1$. These states are normalized such that

$${}_{L'} \langle 1, b; \mathbf{P}', |\mathbf{k}'| | 1, a; \mathbf{P}, |\mathbf{k}\rangle_L = \delta^3(\mathbf{P} - \mathbf{P}') \delta(|\mathbf{k}| - |\mathbf{k}'|) \delta^{ab} \delta^{LL'} \quad . \quad (2.24)$$

Scattering between the S-wave and D-wave is induced by local operators first arising at Q^1 in the power counting. At order Q^1 and Q^2 , the lagrange density describing such interaction is

$$\begin{aligned} \mathcal{L}_2^{(sd)} &= \frac{1}{4} \not{C}_0^{(sd)} \left(N^T P^i N \right)^\dagger \left(N^T \mathcal{O}^{(sd),xyj} N \right) \mathcal{T}^{ijxy} + \text{h.c.} \\ &\quad - \frac{1}{16} \not{C}_2^{(sd)} \left(N^T \left[P_i \overleftrightarrow{\mathbf{D}}^2 + \overleftrightarrow{\mathbf{D}}^2 P_i - 2 \overleftrightarrow{\mathbf{D}} P_i \overleftrightarrow{\mathbf{D}} \right] N \right)^\dagger \left(N^T \mathcal{O}^{(sd),xyj} N \right) \mathcal{T}^{ijxy} + \text{h.c.} \quad , \quad (2.25) \end{aligned}$$

where

$$\begin{aligned} \mathcal{O}^{(sd),xyj} &= \overleftrightarrow{\mathbf{D}}^x \overleftrightarrow{\mathbf{D}}^y P^j + P^j \overleftrightarrow{\mathbf{D}}^x \overleftrightarrow{\mathbf{D}}^y - \overleftrightarrow{\mathbf{D}}^x P^j \overleftrightarrow{\mathbf{D}}^y - \overleftrightarrow{\mathbf{D}}^y P^j \overleftrightarrow{\mathbf{D}}^x \\ \mathcal{T}^{ijxy} &= \left(\delta^{ix} \delta^{jy} - \frac{1}{n-1} \delta^{ij} \delta^{xy} \right) \quad , \quad (2.26) \end{aligned}$$

and where n is the number of spacetime dimensions. When electromagnetic interactions are ignored the operator in eq. (2.26) collapses to

$$\mathcal{O}^{(sd),xyj} \rightarrow P^j \left(\overleftrightarrow{\nabla} - \overleftrightarrow{\nabla} \right)^x \left(\overleftrightarrow{\nabla} - \overleftrightarrow{\nabla} \right)^y \quad , \quad (2.27)$$

which is explicitly Galilean invariant. As the S-D mixing parameter is being computed up to NLO relativistic corrections do not enter. There is another operator with four derivatives that contributes to S-D mixing,

$$\tilde{\mathcal{L}}_2^{(sd)} = -\frac{1}{16} \not{C}_2^{(sd)} \left(N^T P^i N \right)^\dagger \left(N^T \left[(\overleftrightarrow{\mathbf{D}})^2 \mathcal{O}^{(sd),xyj} + \mathcal{O}^{(sd),xyj} (\overleftrightarrow{\mathbf{D}})^2 - 2 \overleftrightarrow{\mathbf{D}}^l \mathcal{O}^{(sd),xyj} \overleftrightarrow{\mathbf{D}}^l \right] N \right) \mathcal{T}^{ijxy} \quad , \quad (2.28)$$

(along with its hermitian conjugate) but it is of order Q^3 and does not contribute at NLO.

The coefficients that appear in eq. (2.26) themselves have an expansion in powers of Q , e.g. $\not{C}_0^{(sd)} = \not{C}_{0,-1}^{(sd)} + \not{C}_{0,0}^{(sd)} + \dots$. Performing a Q expansion on the mixing parameter $\bar{\varepsilon}_1 = \bar{\varepsilon}_1^{(2)} + \bar{\varepsilon}_1^{(3)} + \dots$ it is straightforward to demonstrate that

$$\begin{aligned} \bar{\varepsilon}_1^{(2)}(|\mathbf{k}|) &= \frac{\sqrt{2}}{3} \left(\frac{\not{C}_{0,-1}^{(sd)}}{\not{C}_{0,-1}^{(3S_1)}} \right) \frac{|\mathbf{k}|^3}{\sqrt{\gamma^2 + |\mathbf{k}|^2}} \\ &= -\frac{M_N}{4\pi} (\mu - \gamma) \frac{\sqrt{2}}{3} \not{C}_{0,-1}^{(sd)} \frac{|\mathbf{k}|^3}{\sqrt{\gamma^2 + |\mathbf{k}|^2}} \quad . \quad (2.29) \end{aligned}$$

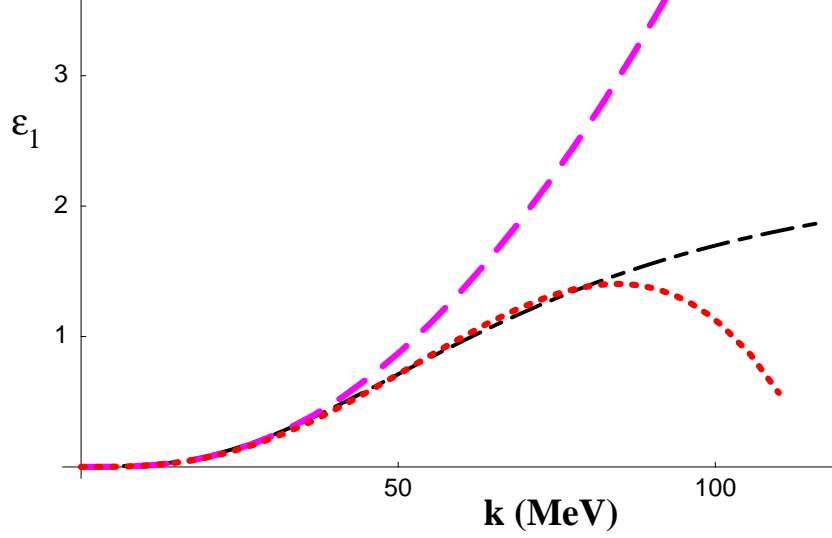


FIG. 2. The S - D mixing parameter $\bar{\varepsilon}_1$ as a function of the center of mass momentum $|\mathbf{k}|$. The dashed curve corresponds to $\bar{\varepsilon}_1^{(2)}$, the dotted curve corresponds to $\bar{\varepsilon}_1^{(2)} + \bar{\varepsilon}_1^{(3)}$, and the dot-dashed curve is the Nijmegen partial wave analysis.

Renormalization group invariance of this leading order contribution to $\bar{\varepsilon}_1$ indicates that $\not{C}_{0,-1}^{(sd)} \propto (\mu - \gamma)^{-1}$. Renormalizing at the scale $\mu = m_\pi$, and comparing with the Nijmegen phase shift analysis [35], we find $\not{C}_{0,-1}^{(sd)} = -3.8 \text{ fm}^4$.

At the next order, Q^3 , the contribution to $\bar{\varepsilon}_1$ is

$$\begin{aligned} \bar{\varepsilon}_1^{(3)}(|\mathbf{k}|) = & -\frac{\sqrt{2}}{3} \frac{M_N}{4\pi} \left[\left(\frac{\mu\gamma\rho_d}{2} \not{C}_{0,-1}^{(sd)} + (\mu - \gamma) \not{C}_{0,0}^{(sd)} \right) \frac{|\mathbf{k}|^3}{\sqrt{\gamma^2 + |\mathbf{k}|^2}} \right. \\ & \left. + \left(\frac{\rho_d}{2} \not{C}_{0,-1}^{(sd)} + (\mu - \gamma) \not{C}_{2,-2}^{(sd)} \right) \frac{|\mathbf{k}|^5}{\sqrt{\gamma^2 + |\mathbf{k}|^2}} \right], \end{aligned} \quad (2.30)$$

where we have expanded $\not{C}_2^{(sd)} = \not{C}_{2,-2}^{(sd)} + \dots$. The first term in eq. (2.30) has the same momentum dependence as $\bar{\varepsilon}_1^{(2)}$, the leading contribution in eq. (2.29). Requiring that the momentum structure of $\bar{\varepsilon}_1^{(2)}$ does not appear at higher orders in the expansion constrains $\not{C}_{0,0}^{(sd)}$ to be

$$\not{C}_{0,0}^{(sd)} = -\frac{\mu\gamma\rho_d}{2(\mu - \gamma)} \not{C}_{0,-1}^{(sd)}. \quad (2.31)$$

Further, as the second term in eq. (2.30) is an observable, we obtain the RG equation

$$\mu \frac{d}{d\mu} \left(\frac{\rho_d}{2} \not{C}_{0,-1}^{(sd)} + (\mu - \gamma) \not{C}_{2,-2}^{(sd)} \right) = 0. \quad (2.32)$$

The only free parameter $\not{C}_{2,-2}^{(sd)} = +18 \text{ fm}^6$, renormalized at $\mu = m_\pi$, is fit to the Nijmegen phase shift analysis [35], as shown in fig. (2).

Local operators that contribute to D-wave to D-wave scattering contain four or more powers of the external momenta. A RG analysis shows that the coefficient of the leading interaction scales like μ^{-1} , through the time-ordered product of two $\not{C}_0^{(sd)}$ operators. Therefore, contributions to the scattering amplitude start at order Q^3 (N⁴LO, i.e. $\delta_2^{(4)}$ is the first non-zero contribution to the δ_2 phase shift), which is higher order than we are working.

III. PROPERTIES OF THE DEUTERON

In the previous section nucleon-nucleon scattering was used to determine the coefficients that appear in EFT($\not{\mathcal{H}}$) up to NNLO for S-wave interactions and up to NLO for mixing between the S-wave and D-wave. This provides us with enough information to determine several properties of the deuteron up to NNLO in EFT($\not{\mathcal{H}}$).

To begin with it is informative to recover basic kinematic properties of the deuteron from the effective field theory formalism. The inclusion of the deuteron into EFT was discussed in detail in [12], but relativistic corrections were not included. In order to compute the matrix element of the electromagnetic current between deuteron states, one starts by defining the 3-point function for two nucleons with kinetic energy T interacting with the electromagnetic current, transferring four-momentum q and producing two nucleons with kinetic energy T' ,

$$G_{ij}^\mu(T, T', q) = \int d^4x d^4y e^{+i(T'x_0 - \mathbf{p}' \cdot \mathbf{x})} e^{-i(Ty_0 - \mathbf{p} \cdot \mathbf{y})} \langle 0 | T [\mathcal{D}_i(x) J_{\text{em}}^\mu(0) \mathcal{D}_j(y)^\dagger] | 0 \rangle \quad . \quad (3.1)$$

where $\mathcal{D}_i(x) = N^T P_i N(x)$. The S-matrix element for this interaction is found by LSZ reduction of this Green-function

$$\langle \mathbf{p}', j | J_{\text{em}}^\mu | \mathbf{p}, i \rangle = \left(\sqrt{Z} \right)^2 \left[G^{-1}(T) G^{-1}(T') G_{ij}^\mu(T, T', q) \right]_{T \rightarrow T_{\text{pole}}, T' \rightarrow T'_{\text{pole}}} \quad , \quad (3.2)$$

where T_{pole} is the location of the deuteron pole for two nucleons moving with three-momentum \mathbf{p} ,

$$\begin{aligned} T_{\text{pole}} + \frac{T_{\text{pole}}^2}{4M_N} - \frac{|\mathbf{p}|^2}{4M_N} &= -\frac{\gamma^2}{M_N} + \frac{\gamma^4}{4M_N^3} \\ T_{\text{pole}} &= -\frac{\gamma^2}{M_N} + \frac{|\mathbf{p}|^2}{4M_N} + \frac{\gamma^2 |\mathbf{p}|^2}{8M_N^3} - \frac{|\mathbf{p}|^4}{64M_N^3} + \dots \quad . \end{aligned} \quad (3.3)$$

The expression for T_{pole} has been expanded in powers of M_N because it is the nucleon mass that will naturally arise from Feynman diagrams computed with the effective field theory. An analogous expression holds for T'_{pole} . The ellipses in eq. (3.3) denote terms of order Q^6 or higher. The two nucleon two-point function, defined in [12] can be generalized to include relativistic effects,

$$G(T) = \int d^4x e^{i(Tx_0 - \mathbf{p} \cdot \mathbf{x})} \langle 0 | T [\mathcal{D}_i(x) \mathcal{D}_j^\dagger(0)] | 0 \rangle = \delta_{ij} \frac{iZ(T)}{T - T_{\text{pole}} + i\epsilon} \quad . \quad (3.4)$$

The wavefunction renormalization factors are straightforward to compute from a single nucleon-nucleon bubble, which is explicitly lorentz invariant (up to the order one computes). An important modification arising from the inclusion of relativistic effects is that

the two-point function is an explicit function of $T + \frac{T^2}{4M_N} - \frac{|\mathbf{p}|^2}{4M_N}$. This leads to wavefunction renormalization factors of

$$Z = \mathcal{Z}(T_{\text{pole}}) = \left[\frac{1 + \frac{T_{\text{pole}}}{2M_N}}{d\Sigma(T)/dT} \right]_{T \rightarrow T_{\text{pole}}}, \quad (3.5)$$

where $\Sigma(T)$ is the irreducible bubble presented in [12]. We find that

$$\#Z = -\frac{8\pi\gamma}{M_N^2} \left[1 + \gamma\rho_d + \gamma^2\rho_d^2 + \frac{\gamma^2(7\mu - 5\gamma)}{8M_N^2(\mu - \gamma)} + \dots \right], \quad (3.6)$$

which is lorentz invariant, but depends on the renormalization scale μ .

Evaluating the matrix element of the Hamiltonian between deuteron states

$$\begin{aligned} \langle \mathbf{p}', j | H | \mathbf{p}, i \rangle &= \langle \mathbf{p}', j | \int d^3x \left[N^\dagger \left(M_N + \frac{\nabla^2}{2M_N} \right) N + \#C_0^{(3S_1)} (N^T P_i N)^\dagger (N^T P_i N) + \dots \right] | \mathbf{p}, i \rangle \\ &= \left(2M_N + \frac{|\mathbf{p}|^2}{4M_N} - \frac{\gamma^2}{M_N} + \dots \right) (2\pi)^3 \delta^3(\mathbf{p} - \mathbf{p}') \delta_{ij} \\ &= \left(M_d + \frac{|\mathbf{p}|^2}{2M_d} + \dots \right) (2\pi)^3 \delta^3(\mathbf{p} - \mathbf{p}') \delta_{ij} \quad . \end{aligned} \quad (3.7)$$

The interactions and relativistic contributions combine together in such a way to reproduce the deuteron energy-momentum relation at the order to which the calculation is being performed. This is a generic feature, which must be present for the theory to be consistent. In computing any observable, one finds that the deuteron mass is recovered order by order in perturbation theory. The issue of gauge invariance for the deuteron bound state is also simply addressed. The lorentz-invariant lagrange density that describes the leading low-energy interactions of the deuteron has the form

$$\mathcal{L} = d_j^\dagger \left[iD_0 + \frac{\mathbf{D}^2}{2M_d} - \frac{D_0^2}{2M_d} \right] d_j + \dots \quad , \quad (3.8)$$

and so reproducing the correct energy-momentum relation for the deuteron order by order in the expansion forces the matrix elements to be gauge invariant order by order in the expansion. In fact, direct calculation including the leading relativistic corrections gives

$$\mathcal{L} = d_j^\dagger \left[i(\partial_0 + ieA_0) + (\nabla - ie\mathbf{A})^2 \left(\frac{1}{4M_N} + \frac{\gamma^2}{8M_N^3} \right) - (\partial_0 + ieA_0)^2 \left(\frac{1}{4M_N} \right) \right] d_j + \dots \quad . \quad (3.9)$$

Order by order one recovers the correct matrix elements of J_{em}^μ to reproduce the couplings induced by eq. (3.8) and also the Thompson limit for photon-deuteron elastic scattering.

A. Electric Polarizability of the Deuteron

The electric polarizability of the deuteron, α_{E0} , has been investigated thoroughly with potential models [37]- [46]. To a very high precision one obtains $\alpha_{E0} = 0.6328 \pm 0.0017 \text{ fm}^3$

with those techniques. This is no surprise because the electric polarizability is dominated by the long range behavior of the deuteron wavefunction. If the model is tuned to reproduce this component of the wavefunction the predicted electric polarizability should be very close to nature. In effective range theory the polarizabilities are assumed to be dominated by the asymptotic S-wave component of the deuteron wave function,

$$\psi^{(\text{ER})}(\mathbf{r}) = \sqrt{\frac{\gamma}{2\pi(1-\gamma\rho_d)}} \frac{e^{-\gamma r}}{r} \quad , \quad (3.10)$$

which yields an electric polarizability of [37,47]

$$\begin{aligned} \alpha_{E0}^{\text{ER}} &= \frac{\alpha M_N}{32\gamma^4} \frac{1}{1-\gamma\rho_d} \\ &= \frac{\alpha M_N}{32\gamma^4} [1 + \gamma\rho_d + \gamma^2\rho_d^2 + \dots] \quad , \end{aligned} \quad (3.11)$$

where α is the electromagnetic fine structure constant. Numerically, $\alpha_{E0}^{\text{ER}} = 0.6338 \text{ fm}^3$, which is very close to the value obtained by the potential model calculations.

With the EFT($\not{\pi}$) we have computed α_{E0} up to NNLO, including relativistic corrections. As with the phase shifts, it has a perturbative expansion in Q , $\alpha_{E0} = \alpha_{E0}^{(-4)} + \alpha_{E0}^{(-3)} + \alpha_{E0}^{(-2)} + \dots$, and we find

$$\begin{aligned} \alpha_{E0}^{(-4)} + \alpha_{E0}^{(-3)} + \alpha_{E0}^{(-2)} &= \frac{\alpha M_N}{32\gamma^4} \left[1 + \gamma\rho_d + \gamma^2\rho_d^2 + \frac{2\gamma^2}{3M_N^2} \right] \\ &= 0.377 + 0.153 + 0.062 + 0.0006 \\ &= 0.592 \text{ fm}^3 \quad . \end{aligned} \quad (3.12)$$

Numerically, the relativistic corrections are very small, two orders of magnitude smaller than the NNLO corrections from the four-nucleon interactions. The value of α_{E0} shown in eq. (3.12) is within $\sim 5\%$ of that computed with potential models and with effective range theory. Despite making a small contribution to the numerical value of α_{E0} this calculation demonstrates that relativistic contributions can be computed easily with the EFT. The operators that mix S-wave and D-wave (corresponding to the D-wave component of the deuteron in potential model language) make contributions to $\alpha_E^{(-2)}$. They do not contribute to the scalar polarizability, $\alpha_{E0}^{(-2)}$, but do contribute to the tensor polarizability, $\alpha_{E2}^{(-2)}$. Such operators will contribute to α_{E0} at higher orders in the expansion.

The four-nucleon operators in the EFT($\not{\pi}$) reproduce the contributions from effective range theory in addition to the relativistic corrections that arise at NNLO. However, the situation is different at higher orders. $\alpha_{E0}^{(-1)}$ will receive contributions from P-wave interaction between nucleons (a two-derivative operator that is not renormalized by the large S-wave scattering length). $\alpha_{E0}^{(0)}$ receives contributions from the polarizability of the nucleons themselves. It is only $\alpha_{E0}^{(1)}$ and higher that receive contributions from the four-nucleon-two-photon interaction, a counterterm for the polarizability of the deuteron, that can only be determined from two-nucleon and two-photon processes. Extrapolating the relative size of the contributions seen in eq. (3.12) we conclude that the counterterm contribution will be of order ~ 0.005 , much larger than the relativistic corrections, but still only $\sim 1\%$.

In the EFT with pions included as a dynamical field, the electric polarizability at NLO is [13]

$$\begin{aligned}
\alpha_{E0} &= \frac{\alpha M_N}{32\gamma^4} \left[1 + C_2(\mu) \frac{M_N \gamma (\mu - \gamma)^2}{2\pi} + \frac{g_A^2 M_N \gamma m_\pi^2 (3m_\pi^2 + 16m_\pi \gamma + 24\gamma^2)}{12\pi f^2 (m_\pi + 2\gamma)^4} \right] \\
&\rightarrow \frac{\alpha M_N}{32\gamma^4} \left[1 + C_2(\mu) \frac{M_N \gamma (\mu - \gamma)^2}{2\pi} + \frac{g_A^2 M_N \gamma}{4\pi f^2} \left(1 - \frac{8}{3} \frac{\gamma}{m_\pi} + \frac{16}{3} \frac{\gamma^2}{m_\pi^2} + \dots \right) \right] \\
&= \frac{\alpha M_N}{32\gamma^4} \left[1 + \gamma \rho_d + \frac{g_A^2 M_N \gamma}{4\pi f^2} \frac{10}{3} \frac{\gamma^2}{m_\pi^2} + \dots \right] , \tag{3.13}
\end{aligned}$$

where g_A is the pion-nucleon axial coupling constant, and f is the pion decay constant. From the expansion of α_{E0} in powers of γ/m_π that appears in eq. (3.13) it is clear that one recovers the effective range expansion, but with an additional contribution from the pions that is higher order in the momentum expansion. In the EFT($\not{\pi}$), $\gamma/m_\pi \sim Q$ while in the theory with dynamical pions it is $\gamma/m_\pi \sim Q^0$. The residual contribution on the third line of eq. (3.13) proportional to g_A^2 is therefore N³LO in the momentum expansion appropriate to the theory without pions.

B. Electric Charge Form-Factor of the Deuteron

The electric charge form factor of the deuteron is a very well measured object over a wide range of momentum transfers. Potential models and effective range theory reproduce the data very well in the kinematic regions where they are applicable. (For a recent and very comprehensive review, see [48].)

A deuteron with four-momentum p^μ and polarization vector ϵ^μ is described by the state $|\mathbf{p}, \epsilon\rangle$, where the polarization vector satisfies $p_\mu \epsilon^\mu = 0$. An orthonormal basis of polarization vectors ϵ_i^μ satisfies

$$p_\mu \epsilon_i^\mu = 0 , \quad \epsilon_{i\mu}^* \epsilon_j^\mu = -\delta_{ij} , \quad \sum_{i=1}^3 \epsilon_i^{*\mu} \epsilon_i^\nu = \frac{p^\mu p^\nu}{M_d^2} - g^{\mu\nu} , \tag{3.14}$$

where M_d is the deuteron mass. It is convenient to choose the basis polarization vectors so that in the deuteron rest frame $\epsilon_i^\mu = \delta_i^\mu$. Deuteron states with these polarizations are denoted by $|\mathbf{p}, i\rangle$ (i.e., $|\mathbf{p}, i\rangle \equiv |\mathbf{p}, \epsilon_i^\mu\rangle$) and satisfy the normalization condition

$$\langle \mathbf{p}', j | \mathbf{p}, i \rangle = (2\pi)^3 \delta^3(\mathbf{p} - \mathbf{p}') \delta_{ij} . \tag{3.15}$$

In terms of these states the nonrelativistic expansion of the matrix element of the electromagnetic current is (up to NNLO)

$$\begin{aligned}
\langle \mathbf{p}', j | J_{em}^0 | \mathbf{p}, i \rangle &= e \left[F_C(q^2) \delta_{ij} + \frac{1}{2M_d^2} F_Q(q^2) \left(\mathbf{q}_i \mathbf{q}_j - \frac{1}{n-1} \mathbf{q}^2 \delta_{ij} \right) \right] \left(\frac{E + E'}{2M_d} \right) , \\
\langle \mathbf{p}', j | \mathbf{J}_{em}^k | \mathbf{p}, i \rangle &= \frac{e}{2M_d} \left[F_C(q^2) \delta_{ij} (\mathbf{p} + \mathbf{p}')^k + F_M(q^2) \left(\delta_j^k \mathbf{q}_i - \delta_i^k \mathbf{q}_j \right) \right. \\
&\quad \left. + \frac{1}{2M_d^2} F_Q(q^2) \left(\mathbf{q}_i \mathbf{q}_j - \frac{1}{n-1} \mathbf{q}^2 \delta_{ij} \right) (\mathbf{p} + \mathbf{p}')^k \right] , \tag{3.16}
\end{aligned}$$

where $\mathbf{q} = \mathbf{p}' - \mathbf{p}$, $q^2 = q_0^2 - |\mathbf{q}|^2$, is the square of the four-momentum transfer, and n is the number of space-time dimensions. (Note that we are using a different normalization of states to [12,49]). The dimensionless form factors defined in eq. (3.16) are normalized such that

$$\begin{aligned} F_C(0) &= 1 \quad , \\ \frac{e}{2M_d} F_M(0) &= \mu_M \quad , \\ \frac{1}{M_d^2} F_Q(0) &= \mu_Q \quad , \end{aligned} \tag{3.17}$$

where $\mu_M = 0.85741 \frac{e}{2M_N}$ is the deuteron magnetic moment, and $\mu_Q = 0.2859 \text{ fm}^2$ is the deuteron quadrupole moment. The charge radius of the deuteron $\sqrt{\langle r_d^2 \rangle}$ is defined by

$$F_C(q^2) = 1 + \frac{1}{6} \langle r_d^2 \rangle q^2 + \dots \quad . \tag{3.18}$$

In effective range theory, the short-distance part of the deuteron wave function is only important for establishing the charge normalization condition, $F_C(0) = 1$. The prediction of effective range theory for the form factor $F_C(q^2)$ follows from the Fourier transform of $|\psi^{(ER)}(\mathbf{r})|^2$,

$$F_C^{(ER)}(q^2) = \left(\frac{1}{1 - \gamma\rho_d} \right) \left(\left(\frac{4\gamma}{\sqrt{-q^2}} \right) \tan^{-1} \left(\frac{\sqrt{-q^2}}{4\gamma} \right) - \gamma\rho_d \right) \quad . \tag{3.19}$$

This yields a deuteron charge radius,

$$\begin{aligned} \langle r_d^2 \rangle^{\text{ER}} &= \frac{1}{8\gamma^2} \frac{1}{1 - \gamma\rho_d} \\ &= \frac{1}{8\gamma^2} \left[1 + \gamma\rho_d + \gamma^2\rho_d^2 + \dots \right] \quad , \end{aligned} \tag{3.20}$$

which gives a numerical value of $\sqrt{\langle r_d^2 \rangle^{\text{ER}}} = 1.98 \text{ fm}$, very close to the quoted value of the matter radius of the deuteron [50,51] of $r_m = 1.967 \pm 0.002 \text{ fm}$. Conventionally, the charge radius is obtained by combining the nucleon charge radius in quadrature with the matter radius, and agrees very well with the experimental value.

In the EFT($\not{\pi}$), the charge form factor $F_C(q^2)$ has an expansion in powers of Q , $F_C(q^2) = F_C^{(0)}(q^2) + F_C^{(1)}(q^2) + F_C^{(2)}(q^2) + \dots$ where the superscript denotes the order of the contribution. The leading contribution to charge form factor $F_C(q^2)$ is calculated to be

$$F_C^{(0)}(q^2) = \frac{4\gamma}{\sqrt{-q^2}} \tan^{-1} \left(\frac{\sqrt{-q^2}}{4\gamma} \right) \quad , \tag{3.21}$$

which reproduces the leading term in a $\gamma\rho_d$ expansion of the form factor computed with effective range, eq. (3.19). At NLO, we find a contribution to the charge form-factor of

$$F_C^{(1)}(q^2) = -\gamma\rho_d \left[1 - \frac{4\gamma}{\sqrt{-q^2}} \tan^{-1} \left(\frac{\sqrt{-q^2}}{4\gamma} \right) \right] \quad , \tag{3.22}$$

which reproduces the subleading term in the $\gamma\rho_d$ expansion of the effective range result, eq. (3.19). At NNLO, there are contributions from several types of graphs, including relativistic corrections. We find

$$\begin{aligned}
F_C^{(2)}(q^2) &= -\gamma^2 \rho_d^2 \left[1 - \frac{4\gamma}{\sqrt{-q^2}} \tan^{-1} \left(\frac{\sqrt{-q^2}}{4\gamma} \right) \right] \\
&+ \frac{1}{M_N^2} \left[\frac{10\gamma^4}{16\gamma^2 - q^2} - \frac{\gamma^2}{2} - \frac{1}{32} (q^2 + 4\gamma^2) \frac{4\gamma}{\sqrt{-q^2}} \tan^{-1} \left(\frac{\sqrt{-q^2}}{4\gamma} \right) \right] \\
&+ \frac{1}{6} \langle r_{N,0}^2 \rangle q^2 \frac{4\gamma}{\sqrt{-q^2}} \tan^{-1} \left(\frac{\sqrt{-q^2}}{4\gamma} \right) \quad , \tag{3.23}
\end{aligned}$$

where the first line of eq. (3.23) reproduces the subsubleading term in the effective range expansion, eq. (3.19), while the second term is the relativistic correction. The third term is the contribution from the isoscalar charge radius of the nucleon, $\sqrt{\langle r_{N,0}^2 \rangle}$, which is measured to be $\sqrt{\langle r_{N,0}^2 \rangle} = 0.79 \pm 0.01$ fm. This measured value contains both relativistic corrections, $\sqrt{\langle r_{N,\text{rel}}^2 \rangle} = \sqrt{\frac{3}{4M_N^2}} = 0.18$ fm (the Foldy term), and contributions from strong interactions. There is no reason to separate these two contributions, as $\langle r_{N,0}^2 \rangle$ is the coefficient of the nucleon-photon charge radius operator in the single nucleon sector.

The charge radius of the deuteron resulting from this form factor is

$$\begin{aligned}
\langle r_d^2 \rangle^{\text{EFT}} &= \langle r_{N,0}^2 \rangle + \frac{1}{8\gamma^2} [1 + \gamma\rho_d + \gamma^2 \rho_d^2] + \frac{1}{32M_N^2} \\
&= 0.62 + 2.33 + 0.95 + 0.39 + 0.0014 \\
&= 4.30 \text{ fm}^2 \quad , \tag{3.24}
\end{aligned}$$

where the last term is the relativistic correction. Taking the square root of this value gives $\sqrt{\langle r_d^2 \rangle} = 2.07$ fm, which is within a few percent of the measured value of $\sqrt{\langle r_d^2 \rangle} = 2.1303$ fm [48,50–52]. The magnitude of the relativistic correction we have computed, $\langle r_{d,\text{rel}}^2 \rangle = +0.0014 \text{ fm}^2$, is the same as the contribution from the spin-orbit interaction (relativistic effect) computed in [51], but is of opposite sign.

A comparison between eq. (3.24) and eq. (3.20) reveals that charge radius computed up to NNLO in EFT($\not{\pi}$) is the same as that computed with effective range theory up to very small relativistic corrections. However, at N³LO there is a contribution to the charge form factor and to the charge radius from a four-nucleon-one-photon operator of the form

$$\mathcal{O}_{\text{ct}} = (N^T P_i N)^\dagger (N^T P_i N) \nabla^2 A_0 \quad . \tag{3.25}$$

Therefore at N³LO the prediction of EFT($\not{\pi}$) and effective range theory will differ.

C. Magnetic Form-Factor of the Deuteron

The magnetic form-factor of the deuteron has been computed in the effective field theory with dynamical pions [12] and is found to be dominated by the nucleon isoscalar magnetic moment. At NLO there are no mesonic corrections other than those that can be absorbed

into the definition of the nucleon magnetic moment. However, there is a contribution from a four-nucleon-one-photon counterterm with an unknown coefficient. As the pions play no explicit role in the deuteron magnetic moment at NLO, one can immediately write an expression for the magnetic moment and form factor in EFT($\not{\tau}$) from the expressions given in [12].

The Lagrange density describing the magnetic interactions of the nucleons is

$$\mathcal{L}_{1,B} = \frac{e}{2M_N} N^\dagger (\kappa_0 + \kappa_1 \tau_3) \boldsymbol{\sigma} \cdot \mathbf{B} N \quad , \quad (3.26)$$

where $\kappa_0 = \frac{1}{2}(\kappa_p + \kappa_n)$ and $\kappa_1 = \frac{1}{2}(\kappa_p - \kappa_n)$ are the isoscalar and isovector nucleon magnetic moments in nuclear magnetons, with

$$\kappa_p = 2.79285 \quad , \quad \kappa_n = -1.91304 \quad . \quad (3.27)$$

The magnetic field is conventionally defined $\mathbf{B} = \nabla \times \mathbf{A}$. At NLO there are four-nucleon-one-photon operators that appear and can contribute to both the deuteron magnetic moment and the rate for $np \rightarrow d\gamma$,

$$\mathcal{L}_{2,B} = \left[e \not{L}_1 (N^T P_i N)^\dagger (N^T \bar{P}_3 N) B_i - e \not{L}_2 i \epsilon_{ijk} (N^T P_i N)^\dagger (N^T P_j N) B_k + \text{h.c.} \right] \quad . \quad (3.28)$$

At NLO the deuteron magnetic moment is

$$\mu_d = \frac{e}{2M_N} \left(\kappa_p + \kappa_n + \not{L}_2 \frac{2M_N \gamma (\mu - \gamma)^2}{\pi} \right) \quad . \quad (3.29)$$

Comparison with the measured value of μ_d gives

$$\not{L}_2(m_\pi) = -0.149 \text{ fm}^4 \quad , \quad (3.30)$$

at the renormalization scale $\mu = m_\pi$. The evolution of the $\not{L}_2(\mu)$ operator as the renormalization scale is changed is determined by the RG equation

$$\mu \frac{d}{d\mu} \left[\frac{\not{L}_2}{(\not{C}_{0,-1}^{(3S_1)})^2} \right] = 0 \quad . \quad (3.31)$$

The magnetic form factor has an expansion in powers of Q , $F_M(q^2) = F_M^{(0)}(q^2) + F_M^{(1)}(q^2) + \dots$. We find that

$$\frac{eF_M^{(0)}(q^2)}{2M_d} = \kappa_0 \frac{e}{M_N} F_C^{(0)}(q^2) = \kappa_0 \frac{e}{M_N} \frac{4\gamma}{\sqrt{-q^2}} \tan^{-1} \left(\frac{\sqrt{-q^2}}{4\gamma} \right) \quad , \quad (3.32)$$

and

$$\begin{aligned} \frac{eF_M^{(1)}(q^2)}{2M_d} &= \kappa_0 \frac{e}{M_N} F_C^{(1)}(q^2) + e \not{L}_2 \frac{\gamma}{\pi} (\mu - \gamma)^2 \\ &= -\kappa_0 \frac{e}{M_N} \gamma \rho_d \left[1 - \frac{4\gamma}{\sqrt{-q^2}} \tan^{-1} \left(\frac{\sqrt{-q^2}}{4\gamma} \right) \right] + e \not{L}_2 \frac{\gamma}{\pi} (\mu - \gamma)^2 \quad . \end{aligned} \quad (3.33)$$

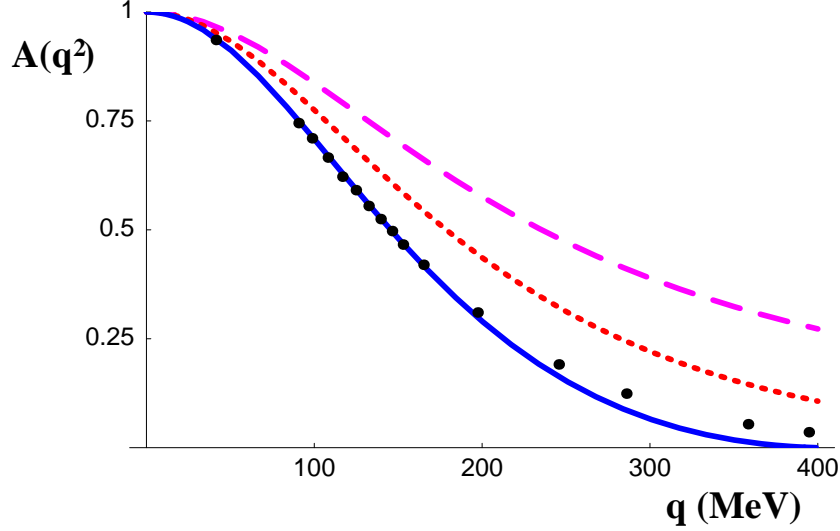


FIG. 3. The form factor $A(q^2)$ as a function of $|\mathbf{q}| = \sqrt{-q^2}$. The dashed curve corresponds to the leading order prediction, the dotted curve corresponds to the next-to-leading order prediction, and the solid curve corresponds to the next-to-next-to-leading order prediction, in EFT(π).

Despite the fact that \not{L}_2 is numerically small, it is important to realize that the effective range expansion for the deuteron magnetic moment is not formally valid beyond leading order (where $\mu_d = \frac{e}{2M_N}(\kappa_p + \kappa_n)$). At NLO, there is a counterterm that is allowed by the symmetries of the theory and it is expected to be of natural size, which in EFT(π) is set by the pion mass. Given that there is a counterterm at NLO, we do not pursue this calculation to higher orders, even though it is straightforward.

It is combinations of the electric, magnetic and quadrupole form factors that are measured in elastic electron-deuteron scattering. The differential cross section for unpolarized elastic electron-deuteron scattering is given by

$$\frac{d\sigma}{d\Omega} = \frac{d\sigma}{d\Omega}\Big|_{\text{Mott}} \left[A(q^2) + B(q^2) \tan^2\left(\frac{\theta}{2}\right) \right] \quad , \quad (3.34)$$

where A and B are related to the form factors that appear in eq. (3.16) by [48]

$$\begin{aligned} A &= F_C^2 + \frac{2}{3}\eta F_M^2 + \frac{8}{9}\eta^2 F_Q^2 \quad , \\ B &= \frac{4}{3}\eta(1 + \eta)F_M^2 \quad , \end{aligned} \quad (3.35)$$

with $\eta = -q^2/4M_d^2$. In order to compare with data, we take our analytic results for the form factors and expand the expression eq. (3.35) in powers of Q . At the order we are working, A is sensitive both the electric and magnetic form factors, while B depends only on the magnetic form factor. The predictions for $A(q^2)$ and $B(q^2)$ along with data are shown in fig. (3) and fig. (4), respectively.

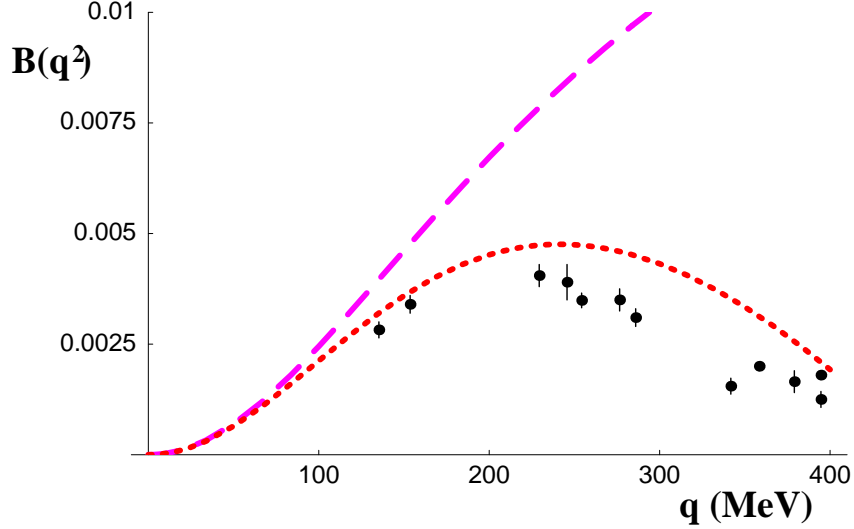


FIG. 4. The form factor $B(q^2)$ as a function of $|\mathbf{q}| = \sqrt{-q^2}$. The dashed curve corresponds to the leading order prediction, and the dotted curve corresponds to the next-to-leading order prediction, in EFT($\not{\pi}$).

D. Electric Quadrupole Form-Factor of the Deuteron

The quadrupole form factor is dominated by mixing between the S-wave and D-wave components of the deuteron due to the NN interaction. However, at subleading orders there are contributions from two-nucleon-one photon operators that do not contribute to nucleon-nucleon scattering (the same as for the deuteron magnetic moment). In the theory with pions, the leading contribution to the quadrupole form factor is from the exchange of a potential pion [12], occurring at NLO in the power counting. The two-loop graphs give

$$\begin{aligned} \frac{F_Q^{(-1)}(|\mathbf{k}|^2)}{M_d^2} &= \frac{3g_A^2 M \gamma}{16\pi f^2 |\mathbf{k}|^3} \int_0^1 dx \frac{1}{x\beta^4 \Delta} \\ &\times \left(\left[3|\mathbf{k}|^2 x^2 (1 + \beta^2)^2 - 24|\mathbf{k}|m_\pi \beta x (1 + \beta^2) + 16m_\pi^2 \beta^2 (3 + \beta^2) \right] \tan^{-1} \beta \right. \\ &\left. + \beta \left[-48m_\pi^2 \beta^2 + 8m_\pi |\mathbf{k}| x \beta (3 + 2\beta^2) - |\mathbf{k}|^2 x^2 (3 + 5\beta^2) \right] \right) \end{aligned} \quad (3.36)$$

where

$$\Delta(x) = \sqrt{\gamma^2 + \frac{1}{4}x(1-x)|\mathbf{k}|^2}, \quad \beta(x) = \frac{|\mathbf{k}|x}{2(\gamma + m_\pi + \Delta)}. \quad (3.37)$$

One finds the quadrupole moment at this order to be

$$\mu_Q^{(-1)} = \frac{g_A^2 M (6\gamma^2 + 9\gamma m_\pi + 4m_\pi^2)}{30\pi f^2 (m_\pi + 2\gamma)^3}. \quad (3.38)$$

Numerically, this is $\mu_Q = \mu_Q^{(-1)} = +0.40 \text{ fm}^2$, about 30% larger than the measured value. This magnitude of deviation is expected based on the size of the expansion parameter.

Subleading contributions, at NNLO in the theory with pions, have been computed in [53]. They depend upon the value of a coefficient that has not yet been determined from nucleon-nucleon scattering in the theory with pions, and so a numerical prediction at this order does not presently exist. Notice, that the expression in eq. (3.38) is of order Q^{-1} in the theory with dynamical pions, but is of order Q^0 in EFT($\not{\pi}$).

In EFT($\not{\pi}$), the contribution from single and multi-pion exchange and from all other meson exchanges to the mixing between the S-wave and D-wave are captured in the $\not{C}_0^{(sd)}$ and $\not{C}_2^{(sd)}$ operators, up to NLO. However, at NLO there is also a contribution from a four-nucleon-one-photon operator, described by the Lagrange density

$$\mathcal{L}_Q = -e \not{C}_Q (N^T P_i N)^\dagger (N^T P_j N) \left(\nabla^i \nabla^j - \frac{1}{n-1} \nabla^2 \delta^{ij} \right) A_0 \quad . \quad (3.39)$$

The operator connects two nucleons in initial and final S-wave states to a D-wave photon.

As we have done with the other form factors, we expand the quadrupole form factor in powers of Q , $F_Q = F_Q^{(0)} + F_Q^{(1)} + \dots$. The leading order form factor is found to be

$$\frac{1}{M_d^2} F_Q^{(0)}(|\mathbf{k}|) = -\not{C}_{0,-1}^{(sd)} \frac{M_N(\mu - \gamma)}{32\pi|\mathbf{k}|^2} \left[-16\gamma^2 + (3|\mathbf{k}|^2 + 16\gamma^2) \frac{4\gamma}{|\mathbf{k}|} \tan^{-1} \left(\frac{|\mathbf{k}|}{4\gamma} \right) \right] \quad . \quad (3.40)$$

At subleading order, we find a contribution to the quadrupole form factor of

$$\begin{aligned} \frac{1}{M_d^2} F_Q^{(1)}(|\mathbf{k}|) = & - \left[\frac{\gamma(\mu - \gamma)^2}{\pi} \not{C}_Q \right. \\ & + \frac{M_N}{2\pi|\mathbf{k}|^2} \left(\frac{\gamma\rho_d}{2} (\mu - \gamma) \not{C}_{0,-1}^{(sd)} - \gamma^2 \left[\frac{\rho_d}{2} \not{C}_{0,-1}^{(sd)} + (\mu - \gamma) \not{C}_{2,-2}^{(sd)} \right] \right) \\ & \left. \left(-\gamma^2 + \left(\frac{3}{16} |\mathbf{k}|^2 + \gamma^2 \right) \frac{4\gamma}{|\mathbf{k}|} \tan^{-1} \left(\frac{|\mathbf{k}|}{4\gamma} \right) \right) \right] \quad , \quad (3.41) \end{aligned}$$

where we have written the form factor in terms of the three-momentum transfer and not the four-momentum transfer as we do not encounter relativistic effects at this order. The expression in eq. (3.41) is written in such a way to make clear that it is RG invariant, using eqs. (2.29) and (2.32).

Numerically, one finds that the quadrupole moment is given by the sum of $\mu_Q^{(0)} = 0.227 \text{ fm}^2$ and $\mu_Q^{(1)} = (0.0812 - 0.0165 \not{C}_Q) \text{ fm}^2$ giving, at NLO,

$$\mu_Q = (0.308 - 0.0165 \not{C}_Q) \text{ fm}^2 \quad , \quad (3.42)$$

where \not{C}_Q is measured in fm^5 . Setting $\not{C}_Q = 0$, we find a quadrupole moment of 0.308 fm^2 , which is to be compared with the measured value of 0.287 fm^2 . In order to reproduce the measured value of the quadrupole moment $\not{C}_Q = +1.34 \text{ fm}^5$, at $\mu = m_\pi$.

In contrast to the electric and magnetic form factors, the quadrupole form factor is found to deviate significantly from calculations in potential models (e.g. the model of [54]) for $|\mathbf{k}| \gtrsim m_\pi$, as shown in fig. (5). However, within the region $|\mathbf{k}| \lesssim m_\pi$ where the EFT($\not{\pi}$) is expected to perturbatively converge to the actual form factor we see deviations of less than $\sim 15\%$, consistent with the size of the expansion parameter. It is clear that a NNLO calculation of this object is required in EFT($\not{\pi}$).

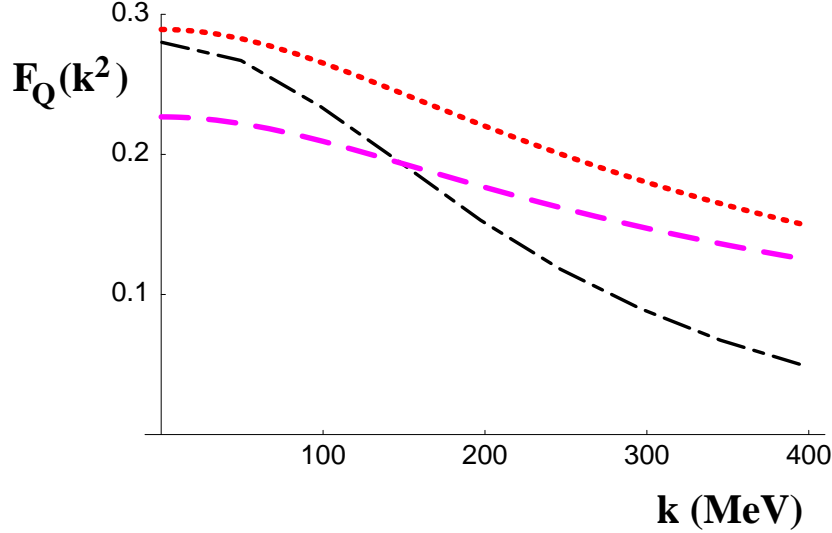


FIG. 5. The quadrupole form factor $F_Q(|\mathbf{k}|^2)$ as a function of $|\mathbf{k}|$. The dashed curve corresponds to the leading order prediction, and the dotted curve corresponds to the next-to-leading order prediction, in EFT($\hat{\pi}$). The dot-dashed curve corresponds to a calculation with the Bonn-B potential in the formulation of [54].

E. The Radiative Capture Process $np \rightarrow d\gamma$

The radiative capture process $np \rightarrow d\gamma$ is a classic nuclear physics demonstration of the existence of meson exchange currents. In addition to the nucleon magnetic moment interactions which dominate this cross section, photons minimally coupled to pions have been estimated to contribute at the $\sim 10\%$ level in various schemes. The cross section for this process was computed in the EFT with KSW power counting in [17], where it was found that the pion exchange current contributions are ultra-violet divergent and require the presence of a counterterm at NLO (it would have been present at NLO even if the graphs were convergent). In EFT($\hat{\pi}$), there are no dynamical mesons, and hence no meson exchange currents. For this process, and all the observables discussed in this paper, the effects of meson exchanges are reproduced order by order by local operators involving multiple nucleon fields. At NLO in EFT($\hat{\pi}$) this corresponds to a single insertion of the \hat{L}_1 operator, defined in eq. (3.28).

The amplitude for the radiative capture of extremely low momentum neutrons $np \rightarrow d\gamma$ has contributions from both the 1S_0 and 3S_1 NN channels. It can be written as

$$i\mathcal{A}(np \rightarrow d\gamma) = e X N^T \tau_2 \sigma_2 [\boldsymbol{\sigma} \cdot \mathbf{k} \boldsymbol{\epsilon}(d)^* \cdot \boldsymbol{\epsilon}(\gamma)^* - \boldsymbol{\sigma} \cdot \boldsymbol{\epsilon}(\gamma)^* \mathbf{k} \cdot \boldsymbol{\epsilon}(d)^*] N \quad (3.43) \\ + ie Y \epsilon^{ijk} \epsilon(d)^{i*} k^j \epsilon(\gamma)^{k*} (N^T \tau_2 \tau_3 \sigma_2 N) \quad ,$$

where $e = |e|$ is the magnitude of the electron charge, N is the doublet of nucleon spinors, $\boldsymbol{\epsilon}(\gamma)$ is the polarization vector for the photon, $\boldsymbol{\epsilon}(d)$ is the polarization vector for the deuteron and \mathbf{k} is the outgoing photon momentum. The term with coefficient X corresponds to capture from the 3S_1 channel while the term with coefficient Y corresponds to capture from the 1S_0 channel. For convenience, we define dimensionless variables \tilde{X} and \tilde{Y} , by

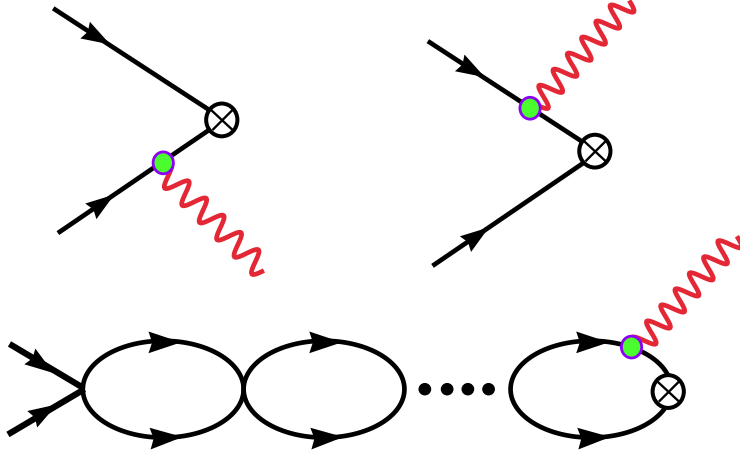


FIG. 6. The Feynman diagrams giving the leading order contribution to $np \rightarrow d\gamma$ in EFT(\hbar). The solid lines denote nucleons and the wavy lines denote photons. The light solid circles correspond to the nucleon magnetic moment coupling of the photon. The crossed circle represents an insertion of the deuteron interpolating field.

$$X = i\frac{2}{M}\sqrt{\frac{\pi}{\gamma^3}}\tilde{X} \quad , \quad Y = i\frac{2}{M}\sqrt{\frac{\pi}{\gamma^3}}\tilde{Y} \quad . \quad (3.44)$$

Both \tilde{X} and \tilde{Y} have the Q expansions, $\tilde{X} = \tilde{X}^{(0)} + \tilde{X}^{(1)} + \dots$, and $\tilde{Y} = \tilde{Y}^{(0)} + \tilde{Y}^{(1)} + \dots$, where a superscript denotes the order in the Q expansion. The capture cross section for very low momentum neutrons with speed $|\mathbf{v}|$ arising from eq. (3.44) is

$$\sigma = \frac{8\pi\alpha\gamma^3}{M^5|\mathbf{v}|} \left[2|\tilde{X}|^2 + |\tilde{Y}|^2 \right] \quad , \quad (3.45)$$

where α is the fine-structure constant.

At leading order in EFT(\hbar) the amplitudes receive contributions from the Feynman diagrams shown in fig. (6) and are

$$\tilde{Y}^{(0)} = \kappa_1 \left(1 - \gamma a^{(1S_0)} \right) \quad , \quad \tilde{X}^{(0)} = 0 \quad , \quad (3.46)$$

where $a^{(1S_0)} = -23.714 \pm 0.013$ fm, is the scattering length in the 1S_0 channel, and κ_1 is the isovector magnetic moment defined in eq. (3.26). At next-to-leading order, NLO, the contribution arising from the Feynman diagrams shown in fig. (7) and fig. (8) is found to be [17]

$$\begin{aligned} \tilde{Y}^{(1)} = & \frac{1}{2}\kappa_1\gamma\rho_d \left(1 - \gamma a^{(1S_0)} \right) \\ & - \frac{M_N}{4\pi}\gamma^2 a^{(1S_0)} (\mu - \gamma) \left(\mu - \frac{1}{a^{(1S_0)}} \right) \left[\not{L}_1 - \frac{\kappa_1\pi}{M_N} \left(\frac{r_0^{(1S_0)}}{\left(\mu - \frac{1}{a^{(1S_0)}} \right)^2} + \frac{\rho_d}{(\mu - \gamma)^2} \right) \right] \quad , \quad (3.47) \end{aligned}$$

where $r_0^{(1S_0)}$ is the effective range in the 1S_0 channel. We have not computed $\tilde{X}^{(1)}$ as it can only contribute at NNLO since $\tilde{X}^{(0)}$ vanishes. The RG evolution of \not{L}_1 was discussed at

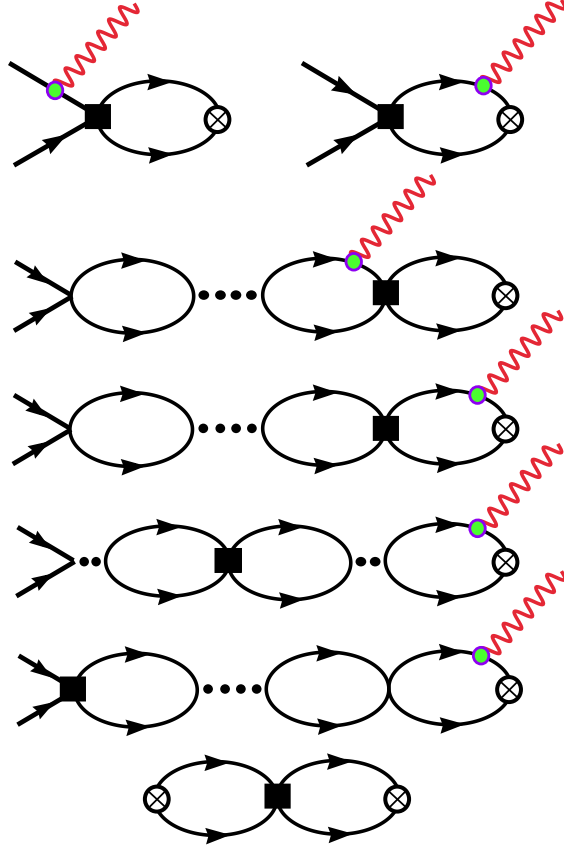


FIG. 7. *Graphs contributing to the amplitude for $n + p \rightarrow d + \gamma$ at subleading order due to insertions of the C_2 operators. The solid lines denote nucleons and the wavy lines denote photons. The light solid circles correspond to the nucleon magnetic moment coupling of the photon. The solid square denotes a C_2 operator. The crossed circle represents an insertion of the deuteron interpolating field. The last graph denotes the contribution from wavefunction renormalization.*

length in [17], where it was made clear that its behavior is much different from \not{L}_2 , the counterterm for the deuteron magnetic moment. In the absence of pions we find

$$\mu \frac{d}{d\mu} \left[\frac{\not{L}_1 - \frac{1}{2} \kappa_1 (\not{C}_{2,-2}^{(3S_1)} + \not{C}_{2,0}^{(1S_0)})}{\not{C}_{0,-1}^{(1S_0)} \not{C}_{0,-1}^{(3S_1)}} \right] = 0 \quad , \quad (3.48)$$

in order that the cross section for $NN \rightarrow NN\gamma$ with the initial nucleons in the $1S_0$ channel and the final nucleons in the $3S_1$ channel be independent of the renormalization scale at all energies. The analytic structure of the amplitude ensures that the capture cross section will be μ -independent, if $NN \rightarrow NN\gamma$ is μ -independent.

The cross section for this process has been measured very precisely for an incident neutron speed of $|\mathbf{v}| = 2200$ m/s to be $\sigma^{\text{expt}} = 334.2 \pm 0.5$ mb [55]. In EFT($\not{\pi}$) we find a cross section at NLO, at this incident neutron speed, of

$$\sigma_{\not{\pi}} = \left(287.1 + 6.51 \not{L}_1 \right) \text{ mb} \quad , \quad (3.49)$$

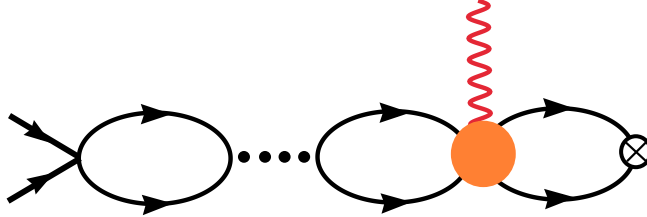


FIG. 8. Local counterterm contribution to the amplitude for $n + p \rightarrow d + \gamma$ at NLO. The solid lines denote nucleons and the wavy lines denote photons. The solid circle corresponds to an insertion of the \not{L}_1 operator. The crossed circle represents an insertion of the deuteron interpolating field.

where \not{L}_1 is in units of fm^4 and is renormalized $\mu = m_\pi$. Requiring $\sigma_\#$ to reproduce the measured cross section σ^{expt} fixes $\not{L}_1 = 7.24 \text{ fm}^4$.

We see that even in the theory without dynamical pions, one is able to recover the cross section for radiative neutron capture at higher orders. It is clear that in this theory the four-nucleon-one-photon operators play a central role in reproducing the low energy observables. In the theory with pions, one can see by examining the contributing Feynman diagrams [17], that in the limit that the momentum transferred to the photon is small the pion propagators can be replaced by $1/m_\pi^2$, while keeping the derivative structure in the numerator. This contribution, as well as the contribution from all hadronic exchanges, is reproduced order by order in the momentum expansion by the contributions from local multi-nucleon-photon interactions. From the calculations in the theory with dynamical pions, the value of \not{L}_1 is not saturated by pion exchange currents as these contributions are divergent, and require the presence of the L_1 operator [17]. Therefore, estimates of \not{L}_1 based on meson exchanges alone are model dependent.

The effective range calculation of $np \rightarrow d\gamma$ was first performed by Bethe and Longmire [32] and revisited by Noyes [56]. After correcting the typographical errors in the expression for σ that appears in the Noyes article, the expressions in the two papers [32,56] are identical,

$$\sigma^{\text{(ER)}} = \frac{2\pi\alpha \kappa_1^2 \gamma^6 (a^{(1S_0)})^2 a^{(3S_1)}}{|\mathbf{v}|M_N^5 (2 - \gamma a^{(3S_1)})} \left(1 + \frac{1}{\gamma a^{(3S_1)}} - \frac{2}{\gamma a^{(1S_0)}} - \frac{1}{2}\gamma r_0^{(1S_0)} \right)^2, \quad (3.50)$$

which when expanded in powers of Q is

$$\sigma^{\text{(ER)}} = \frac{8\pi\alpha\gamma^3}{|\mathbf{v}|M_N^5} \left[\kappa_1^2 (1 - \gamma a^{(1S_0)})^2 + \frac{1}{2}\gamma (\rho_d - r_0^{(1S_0)}) \kappa_1^2 (1 - \gamma a^{(1S_0)})^2 + \frac{1}{2}\gamma (\rho_d + r_0^{(1S_0)}) \kappa_1^2 (1 - \gamma a^{(1S_0)}) + \dots \right]. \quad (3.51)$$

From this expansion, one finds that

$$\tilde{Y}^{\text{ER},(0)} = \kappa_1 (1 - \gamma a^{(1S_0)}) \quad , \quad \tilde{X}^{\text{ER},(0)} = 0 \quad , \quad (3.52)$$

and

$$\tilde{Y}^{\text{ER},(1)} = \frac{1}{4}\kappa_1\gamma (\rho_d - r_0^{(1S_0)}) (1 - \gamma a^{(1S_0)}) + \frac{1}{4}\kappa_1\gamma (\rho_d + r_0^{(1S_0)}) \quad . \quad (3.53)$$

At LO in the EFT($\not{\pi}$) expansion the cross sections agree, however, at NLO the expressions are very different. In addition to the counterterm that appears at this order in the EFT($\not{\pi}$), the contributions from the effective range parameters are found to disagree. In the EFT($\not{\pi}$) the local counterterm is renormalized by the short-distance behavior of graphs involving the C_2 operators and hence the effective range parameters in both channels. Given, this behavior it is no surprise that the effective range contributions differ between the two calculations. Given the explicit μ -dependence in $\tilde{Y}^{(1)}$ and the absence of such dependence in $\tilde{Y}^{\text{ER},(1)}$ it is amusing to ask if there is a scale for which the expressions are identical, with $\not{L}_1 = 0$. Indeed such a scale exists,

$$\mu^{\text{ER}} = \frac{\gamma r_0^{(1S_0)} a^{(1S_0)} - \rho_d}{a^{(1S_0)} (r_0^{(1S_0)} - \rho_d)} \quad , \quad (3.54)$$

which, by inserting the appropriate values, gives scale $\mu^{\text{ER}} \sim 144$ MeV, coincidentally close to $\mu = m_\pi$.

IV. CONCLUSIONS

An effective field theory without dynamical pions can describe all low-energy two-nucleon processes, and generally all multi-nucleon processes. We have shown in detail how EFT($\not{\pi}$) systematically reproduces nucleon-nucleon scattering and the interactions of the deuteron. Effective range theory is seen to emerge as the uncontrolled approximation to EFT($\not{\pi}$) where the multi-nucleon-external current local operators are neglected. For most observables, this is a small effect, while for the radiative capture process $np \rightarrow d\gamma$ this omission gives rise to deviations at the 10% level, which has been known for decades. Inclusion of the local four-nucleon-one-magnetic-photon interaction which enters at NLO in EFT($\not{\pi}$) introduces a free parameter \not{L}_1 , which can be fit to reproduce the measured cross section. As a consequence of this ultra-violet behavior, the NLO contribution to the cross section in EFT($\not{\pi}$) with $\not{L}_1 = 0$ is unrelated to that determined by effective range theory with the simple neglect of such contributions. While this does not satisfy our desire to make a parameter free prediction for this cross section beyond leading order, it does allow us to rigorously relate S-matrix elements for different processes based solely on the symmetries of QCD. The deuteron magnetic moment is another example of an observable where a counter term \not{L}_2 appears at NLO, but numerically this is found to be small.

In working to higher orders in EFT($\not{\pi}$) one encounters relativistic effects, starting at NNLO. The contribution of relativistic effects on nucleon-nucleon scattering, the electric charge form factor of the deuteron and the electric polarizability of the deuteron were calculated at leading order. Their impact upon the static properties of the deuteron are expected to be very small, of order $\sim \gamma^2/M_N^2$, and this was recovered.

We should take a moment to ask about the impact this work will have on our understanding of potential model approaches to nucleon interactions. As we have emphasized, for most processes the effective range expansion provides a relatively good approximation. For some of the observables, such as the deuteron charge radius and the electric polarizability, this arises because counterterms only appear at very high orders in the momentum expansion, while for others, such as the $np \rightarrow d\gamma$, and the deuteron quadrupole moment, there

is a four-nucleon-one-photon counterterm that prevents effective range theory from doing better than $\sim 10\%$. Such counterterms cannot be fixed by the nucleon-nucleon scattering amplitude no matter how precisely it is measured, but they can be determined from inelastic scattering processes. Thus, multi-nucleon processes involving external currents receive contributions from interactions beyond those related by gauge invariance to the nucleon-nucleon interaction. The form and magnitude of such interactions will, in general, depend explicitly upon the choice of the nucleon-nucleon interaction, as is made clear by the RG behavior of the 4L_1 counterterm.

We thank D. Phillips for many useful discussions and for providing us with the calculation of the quadrupole form factor in the formulation of [54] using the Bonn-B potential, that appears in fig. (5). We would like to thank David Kaplan and Mark Wise for several interesting discussions. This work is supported in part by the U.S. Dept. of Energy under Grants No. DE-FG03-97ER4014.

REFERENCES

- [1] S. Weinberg, *Phys. Lett. B* **251**, 288 (1990); *Nucl. Phys. B* **363**, 3 (1991); *Phys. Lett. B* **295**, 114 (1992).
- [2] C. Ordonez and U. van Kolck, *Phys. Lett. B* **291**, 459 (1992); C. Ordonez, L. Ray and U. van Kolck, *Phys. Rev. Lett.* **72**, 1982 (1994); *Phys. Rev. C* **53**, 2086 (1996); U. van Kolck, *Phys. Rev. C* **49**, 2932 (1994).
- [3] J. Friar, nucl-th/9601012; nucl-th/9601013; *Few Body Systems Suppl.* **99**, 1 (1996); nucl-th/9804010; J.L. Friar, D. Huber, and U. van Kolck, *Phys. Rev. C* **59**, 53 (1999).
- [4] T.S. Park, D.P. Min and M. Rho, *Phys. Rev. Lett.* **74**, 4153 (1995) ; *Nucl. Phys. A* **596**, 515 (1996).
- [5] T.D. Cohen, *Phys. Rev. C* **55**, 67 (1997). D.R. Phillips and T.D. Cohen, *Phys. Lett. B* **390**, 7 (1997). K.A. Scaldeferri, D.R. Phillips, C.W. Kao and T.D. Cohen, *Phys. Rev. C* **56**, 679 (1997). S.R. Beane, T.D. Cohen and D.R. Phillips, nucl-th/9709062; D.R. Phillips, S.R. Beane and T.D. Cohen, *Annals Phys.* **263**, 255 (1998).
- [6] M.J. Savage, *Phys. Rev. C* **55**, 2185 (1997).
- [7] G.P. Lepage, nucl-th/9706029, Lectures at 9th Jorge Andre Swieca Summer School: Particles and Fields, Sao Paulo, Brazil, Feb 1997.
- [8] M. Luke and A.V. Manohar, *Phys. Rev. D* **55**, 4129 (1997).
- [9] D.B. Kaplan, M.J. Savage, and M.B. Wise, *Nucl. Phys. B* **478**, 629 (1996).
- [10] D.B. Kaplan, M.J. Savage and M.B. Wise, *Phys. Lett. B* **424**, 390 (1998); *Nucl. Phys. B* **534**, 329 (1998).
- [11] U. van Kolck, *Nucl. Phys. A* **645**, 273 (1999)
- [12] D.B. Kaplan, M.J. Savage and M.B. Wise, nucl-th/9804032, to appear in *Phys. Rev. C*.
- [13] J.W. Chen, H. W. Griesshammer, M. J. Savage and R. P. Springer, *Nucl. Phys. A* **644**, 221 (1999); *Nucl. Phys. A* **644**, 245 (1999).
- [14] J.W. Chen, nucl-th/9810021.
- [15] M. J. Savage and R.P. Springer, *Nucl. Phys. A* **644**, 235 (1999).
- [16] D. B. Kaplan, M. J. Savage, R. P. Springer and M. B. Wise, nucl-th/9807081.
- [17] M. J. Savage, K. A. Scaldeferri, Mark B.Wise, nucl-th/9811029.
- [18] T. Mehen and I.W. Stewart, nucl-th/9901064; nucl-th/9809095; *Phys. Lett. B* **445**, 378 (1999).
- [19] G. Rupak and N. Shoresh, *Private Communication*.
- [20] J. Gegelia, *Phys. Lett. B* **429**, 227 (1998); nucl-th/9806028; nucl-th/9805008; nucl-th/9802038;
- [21] A. K. Rajantie, *Nucl. Phys. B* **480**, 729 (1996).
- [22] J.V. Steele and R.J. Furnstahl, *Nucl. Phys. A* **637**, 46 (1998); nucl-th/9808022.
- [23] T.D. Cohen and J.M. Hansen, *Phys. Rev. C* **59**, 13 (1999); nucl-th/9901065.
- [24] T.-S. Park, K. Kubodera, D.-P. Min, and M. Rho, nucl-th/9807054; astro-ph/9804144; *Phys. Rev. C* **58**, 637 (1998).
- [25] X. Kong and F. Ravndal, nucl-th/9803046; nucl-th/9811076.
- [26] X. Kong and F. Ravndal, *Private Communication*.
- [27] E. Epelbaum and U.G. Meissner, nucl-th/9902042; E. Epelbaum, W. Glockle, A. Kruger and Ulf-G. Meissner, *Nucl. Phys. A* **645**, 413 (1999); E. Epelbaum, W. Glockle

- and Ulf-G. Meissner, *Phys. Lett. B* **439**, 1 (1998); E. Epelbaum, W. Glockle and Ulf-G. Meissner, *Nucl. Phys. A* **637**, 107 (1998).
- [28] T. Mehen, I. W. Stewart and M.B. Wise, hep-ph/9902370.
- [29] D. R. Phillips, S. R. Beane and M. C. Birse, hep-ph/9810049.
- [30] M. N. Butler and J. W. Chen, *Private Communication*.
- [31] P.F. Bedaque, H.W. Hammer and U. van Kolck, *Phys. Rev. Lett.* **82**, 463 (1999); *Phys. Rev. C* **58**, R641 (1998); P.F. Bedaque and U. van Kolck, *Phys. Lett. B* **428**, 1998 (.)
- [32] H. A. Bethe, *Phys. Rev.* **76**, 38 (1949); H. A. Bethe and C. Longmire, *Phys. Rev.* **77**, 647 (1950).
- [33] J.J. de Swart, C.P.F. Terheggen and V.G.J. Stoks, nucl-th/9509032.
- [34] H. P. Stapp, T. J. Ypsilantis and N. Metropolis, *Phys. Rev.* **105**, 302 (1957).
- [35] V.G.J. Stoks, R.A.M. Klomp, C.P.F. Terheggen and J.J. de Swart, *Phys. Rev.* **C49** (1994) 2950, nucl-th/9406039.
- [36] M. Luke and M. J. Savage, *Phys. Rev. D* **57**, 413 (1998).
- [37] J.L. Friar and S. Fallieros, *Phys. Rev. C* **29**, 232 (1984).
- [38] K. Pachucki, D. Liebfried and T.W. Hansch, *Phys. Rev. A* **48**, R1 (1993). K. Pachucki, M. Weitz and T.W. Hansch, *Phys. Rev. A* **49**, 2255 (1994).
- [39] W. Leidemann and R. Rosenfelder, *Phys. Rev. C* **51**, 427 (1995).
- [40] Y. Lu and R. Rosenfelder, *Phys. Lett. B* **319**, 7 (1993).
- [41] J. Martorell, D.W.L. Sprung and D.C. Zheng, *Phys. Rev. C* **51**, 1127 (1995).
- [42] A.I. Milshtein, I.B. Kriplovich and S.S. Petrosyan, *Sov. Phys. JETP* **82**, 616 (1996).
- [43] J.L. Friar and G.L. Payne, *Phys. Rev. C* **55**, 2764 (1997).
- [44] M.I. Levchuk and A.I. L'vov, *Few Body Systems Suppl.* **9**, 439 (1995).
- [45] T. Wilbois, P. Wilhelm and H. Arenhovel, *Few Body Systems Suppl.* **9**, 263 (1995).
- [46] A.V. Karchenko, *Ukr. J. of Phys.* **42**, 18 (1997).
- [47] J.G. Lucas and M.L. Rustgi, *Nucl. Phys. A* **112**, 503 (1968).
- [48] C. W. Wong, *Int. J. of Mod. Phys.* **E3**, 821 (1994).
- [49] J.L. Friar, *Ann. of Phys.* **81**, 332 (1973).
- [50] A.J. Buchmann, H. Henning and P.U. Sauer, *Few-Body Systems*, **21** (1996) 149.
- [51] J. L. Friar, J. Martorell and D. W. L. Sprung, *Phys. Rev. A* **56**, 4579 (1997).
- [52] T. Ericson and W. Weise, *Pions and Nuclei*, Oxford University Press (1988).
- [53] M. Binger, nucl-th/9901012.
- [54] J. Adam Jr. , H. Göller and H. Arenhövel, *Phys. Rev. C* **48**, 370 (1993).
- [55] A.E. Cox, S.A.R. Wynchank and C.H. Collie, *Nucl. Phys.* **74**, 497 (1965).
- [56] H. P. Noyes, *Nucl. Phys.* **74**, 508 (1965).